Brightness Temperatures From Layered Lossy Medium With Rough Surfaces by Combining FDTD and Coherent Methods

Zhi-Hong Lai and Jean-Fu Kiang

***Abstract*— The brightness temperatures from layered lossy medium with rough surfaces, where the physical temperature varies with depth, are computed by using the coherent method, with the field distribution computed by using the finite difference time domain method. The major contribution of the proposed method lies in its flexibility to compute the brightness temperatures from a layered medium with rough interfaces and spatially varying physical temperature. The brightness temperatures from a half-space lossy medium are validated by comparing with data in the literature, and the maximum error of the simulation results, as compared with the literature, is 4.7 K (1.6%), which is slightly above the threshold of 1%.**

***Index Terms*— Brightness temperature, coherent method, finite-difference time-domain (FDTD) method, layered medium, rough surface.**

I. Introduction

BRIGHTNESS temperatures measure the contribution of emissions from the atmosphere [1], [2], vegetation [3], [4], and soils [5]. In the Soil Moisture and Ocean Salinity mission [6] and the Soil Moisture Active and Passive mission [7], the brightness temperatures in L-band (1.41 GHz) were measured for the estimation of soil moisture. The brightness temperatures are determined by soil and vegetation temperatures, surface roughness, soil texture, and moisture. The contribution of other factors than soil moisture itself tends to compromise the accuracy of soil moisture estimation. The soil permittivity is related to the soil moisture [8]. In typical passive remote sensing, the soil permittivity is estimated first, from which the soil moisture is retrieved [9], [10]. For example, the equation in the τ–ω model [11] is helpful for retrieving the soil moisture [9], [10], [12]. The thermal emission from soil is sensitive to the moisture content therein, but is less sensitive to the cloud cover and surface vegetation in the microwave band, especially at longer wavelengths. Thus, the brightness temperatures attributed to the soil are the key parameters for estimating the soil moisture.

Manuscript received October 18, 2018; revised December 7, 2018; accepted January 11, 2019. Date of publication February 7, 2019; date of current version June 24, 2019. This work is sponsored by the Ministry of Science and Technology, Taiwan, under Contract MOST 106-2221-E-002-014. *(Corresponding author: Jean-Fu Kiang.)*

The authors are with the Graduate Institute of Communication Engineering, National Taiwan University, Taipei 10617, Taiwan (e-mail: jfkiang@ntu.edu.tw).

Color versions of one or more of the figures in this letter are available online at http://ieeexplore.ieee.org.

Digital Object Identifier 10.1109/LGRS.2019.2893255

Surface roughness [13], [14] and texture [15], [16] of soil affect the brightness temperatures. Radiative transfer theory has been applied to model active remote sensing of a layered random medium with rough surfaces [17], [18]. The boundary condition between the two adjacent layers represents the specific intensity radiated in a given direction in terms of the scattered specific intensities from all possible directions. Different methods have been proposed to solve the scattering problems involving rough surfaces, including small perturbation method (SPM) [19], extended boundary condition method (EBCM) [20], stabilized EBCM (SEBCM) [21], [22] method of moments (MoMs) [23], radiative transfer (RT) theory [17], [18], [24], and advanced integral equation method (AIEM) [25].

Different challenges may restrain the applicability of these useful methods to some extent. For example, the SPM is limited to the surfaces of small roughness [19], the EBCM may become unstable as the root-mean-square (rms) height of a rough surface is too large, and 3-D EBCM and SEBCM must be implemented in conjunction with periodic boundary conditions. The stability of SEBCM is affected by the medium loss and layer thickness [21]. As the medium loss increases, the field within the medium decays faster with the propagation distance, reducing the magnitude of the observed field and, hence, the accuracy of the solution. The accuracy of the solution may be affected by the number of layers due to accumulation errors. The MoM takes enormous computational time to solve volume integral equations. The RT theory does not provide information on coherent fields.

Analytical scattering models such as AIEM [25] was proposed to compute the soil emissivity, assuming the physical temperature was constant. Typical scattering model computes the emissivity from the soil, which is one minus the reflectivity, then multiplies the emissivity by the constant physical temperature of soil to obtain the brightness temperature. The brightness temperatures from a layered medium with physical temperature varying with depth can be computed by using incoherent RT method and coherent-wave method [24]. The layered RT theory is restricted to slightly absorptive layered media, in which the propagation angles of specific intensities are well defined [24]. If the layered medium is very lossy, as in moistured soils, the specific intensities become diffusive, degrading the accuracy of the layered RT theory. Conventional definition, in terms of far fields, of bistatic scattering and transmission coefficients (BSCs/BTCs), which are

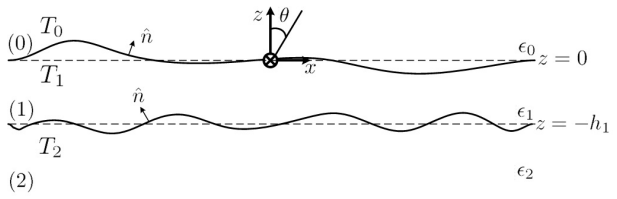

Fig. 1. Schematic of a two-layered medium with rough surfaces.

used to characterize the scattering and transmission, respectively, of specific intensity at rough interfaces of a layered medium [18], [26], may not be applicable in very lossy media in which the far fields vanish. The coherent method is based on the fluctuation dissipation theorem, where the thermal motion in a dissipative medium is attributed to a fluctuating current source $\bar{J}(\bar{r},\omega)$, and its radiated field $\bar{E}(\bar{r},\omega)$ can be represented in terms of the dyadic Green's function $\bar{\bar{G}}(\bar{r},\bar{r}')$.

The major contribution of the proposed method lies in its flexibility to compute the brightness temperatures from a layered medium with rough interfaces and spatially varying physical temperature. The brightness temperatures have been computed by using RT theory (incoherent method), coherent method, or scattering models like SPM, small-slope approximation, AIEM, and so on, to compute the emissivity (which is one minus reflectivity) first then multiplied by a constant physical temperature. The scattering models cannot be applied if the physical temperature is not constant. The coherent method can be used to compute the brightness temperatures from layered soils with spatially varying physical temperature. However, it can only be applied to layered media with flat interfaces due to the difficulty of deriving Green's functions in the presence of rough interfaces. On the other hand, the finite difference time domain (FDTD) method has the flexibility to compute the fields in layered media with rough interfaces. Taking the above-mentioned factors into consideration, the proposed method brings out innovation to compute the field distribution in layered media with rough interfaces and then use the field distribution in the coherent method to compute the brightness temperatures.

In this letter, the field distribution in a layered lossy medium is computed by using the FDTD method [27], [28], and the coherent method is applied to compute the brightness temperatures from the lossy medium. The brightness temperatures from a half-space are used to validate the proposed method, and those from a two-layered lossy medium with rough surfaces are also presented. This letter is organized as follows. The coherent method with field distribution computed via FDTD method is presented in Section II, simulations on layered moistured soils are presented in Section III, and some conclusions are drawn in Section IV.

II. Coherent Method With Field Distribution via FDTD Method

Fig. 1 shows the schematic of a two-layered medium with rough surfaces. By applying the fluctuation dissipation theorem, the brightness temperatures can be represented as [24, Ch. 3]

$$\begin{bmatrix} T_{bv}(\hat{o}) \\ T_{bh}(\hat{o}) \end{bmatrix} = \lim_{r_0\to\infty} \frac{16\pi^2\eta_0\, r_0^2}{A\cos\theta_0} \sum_{\ell=1}^{2} \iiint dxdydz\omega\epsilon_\ell''(z)T_\ell(z) \times \begin{bmatrix} \hat{v}(\hat{o})\cdot\bar{\bar{G}}_{\ell 0}^{t}(\bar{r},\bar{r}_0)\cdot\bar{\bar{G}}_{\ell 0}^{*}(\bar{r},\bar{r}_0)\cdot\hat{v}(\hat{o}) \\ \hat{h}(\hat{o})\cdot\bar{\bar{G}}_{\ell 0}^{t}(\bar{r},\bar{r}_0)\cdot\bar{\bar{G}}_{\ell 0}^{*}(\bar{r},\bar{r}_0)\cdot\hat{h}(\hat{o}) \end{bmatrix} \quad (1)$$

where $\bar{\bar{G}}_{\ell 0}(\bar{r},\bar{r}_0)$ is the dyadic Green's function. Consider a point current source $\bar{J}_p$ with polarization $\hat{p}=\hat{h},\hat{v}$ placed at $\bar{r}_0$ in region (0)

$$\bar{J}_p(\bar{r}) = \hat{p}\delta(\bar{r}-\bar{r}_0). \quad (2)$$

The electric field in layer (ℓ) radiated by $\bar{J}_p$ can be represented in terms of the dyadic Green's function as

$$\bar{E}_{\ell p}(\bar{r}) = -j\omega\mu_0 \iiint d\bar{r}'\bar{\bar{G}}_{\ell 0}(\bar{r},\bar{r}')\cdot\bar{J}_p(\bar{r}'). \quad (3)$$

By substituting (2) into (3), we have

$$\bar{E}_{\ell p}(\bar{r}) = -j\omega\mu_0\bar{\bar{G}}_{\ell 0}(\bar{r},\bar{r}_0)\cdot\hat{p}$$

which implies that

$$|\bar{E}_{\ell p}(\bar{r})|^2 = \omega^2\mu_0^2\hat{p}\cdot\bar{\bar{G}}_{\ell 0}^{t}(\bar{r},\bar{r}_0)\cdot\bar{\bar{G}}_{\ell 0}^{*}(\bar{r},\bar{r}_0)\cdot\hat{p}.$$

Then, (1) can be rewritten as

$$\begin{bmatrix} T_{bv}(\hat{o}) \\ T_{bh}(\hat{o}) \end{bmatrix} = \lim_{r_0\to\infty} \frac{16\pi^2\eta_0\, r_0^2}{\omega\mu_0^2\, A\cos\theta_0} \times \sum_{\ell=1}^{2} \iiint dxdydz\epsilon_\ell''(z)T_\ell(z) \begin{bmatrix} |\bar{E}_{\ell v}(\bar{r})|^2 \\ |\bar{E}_{\ell h}(\bar{r})|^2 \end{bmatrix}. \quad (4)$$

The incident field near the rough surface, radiated by $\bar{J}_p(\bar{r})$, is

$$\bar{E}_{ip}(\bar{r}) = \hat{p}\frac{-j\omega\mu_0 e^{-jk_0r_0}}{4\pi r_0}e^{-jk_0\hat{k}_{0i}\cdot\bar{r}}$$

which can be represented as a uniform plane wave (UPW)

$$\bar{E}'_{ip}(\bar{r}) = \hat{p}E_0e^{-jk_0\hat{k}_{0i}\cdot\bar{r}}.$$

Then, the field in layer (ℓ) is linearly scaled to

$$\bar{E}'_{\ell p}(\bar{r}) = \frac{E_0 4\pi r_0}{-j\omega\mu_0 e^{-jk_0r_0}}\bar{E}_{\ell p}(\bar{r}). \quad (5)$$

By substituting (5) into (4), we have

$$\begin{bmatrix} T_{bv}(\hat{o}) \\ T_{bh}(\hat{o}) \end{bmatrix} = \frac{\omega}{2\ P_{\text{inc}}} \times \sum_{\ell=1}^{2} \iiint dxdydz\epsilon_\ell''(z)T_\ell(z) \begin{bmatrix} |\bar{E}'_{\ell v}(\bar{r})|^2 \\ |\bar{E}'_{\ell h}(\bar{r})|^2 \end{bmatrix} \quad (6)$$

where $P_{\text{inc}} = |E_0|^2\ A\cos\theta_0/(2\eta_0)$ is the incident power upon the rough surface.

In the FDTD scheme [27], [28], the incident wave takes the form of a tapered plane wave (TPW)

$$\bar{E}'_{ip}(\bar{r}) = \hat{p}E_0 e^{-jk_0\hat{k}_{0i}\cdot\bar{r}} G_{\text{tap}}(\bar{r})$$

where

$$G_{\text{tap}}(\bar{r}) = e^{-d_\theta^2(\bar{r},\hat{k}_{0i})/(2r_{0a}^2)} e^{-d_\phi^2(\bar{r},\hat{k}_{0i})/(2r_{0b}^2)}$$
$$r_{0a} = \frac{L_x\cos\theta_0}{\sqrt{-8\ln a}}, \quad r_{0b} = \frac{L_y}{\sqrt{-8\ln a}}$$
$$d_\theta(\bar{r},\hat{k}_{0i}) = |\bar{r}\cdot\hat{\theta}|, \quad d_\phi(\bar{r},\hat{k}_{0i}) = |\bar{r}\cdot\hat{\phi}|.$$

The incident power upon the rough surface enclosed in the computational domain is

$$P_{\text{inc}} = -\frac{|E_0|^2}{2\eta_0}\iint_S ds G_{\text{tap}}^2(\bar{r})\hat{k}_{0i}\cdot\hat{n} = \frac{|E_0|^2}{2\eta_0}U_a(\hat{k}_{0i}) \tag{7}$$

where $\hat{n}$ is the upward surface normal, and

$$U_a(\hat{k}_{0i}) = -\iint_S ds G_{\text{tap}}^2(\bar{r})\hat{k}_{0i}\cdot\hat{n}.$$

By substituting (7) into (6), the brightness temperatures are computed, under an incident TPW, as

$$\begin{bmatrix} T_{bv}(\hat{o}) \\ T_{bh}(\hat{o}) \end{bmatrix} = \frac{\omega\eta_0}{|E_0|^2\ U_a(\hat{k}_{0i})} \times \sum_{\ell=1}^{2}\iiint d\bar{r}\epsilon''_\ell(z)T_\ell(z)\begin{bmatrix} |\bar{E}'_{\ell v}(\bar{r})|^2 \\ |\bar{E}'_{\ell h}(\bar{r})|^2 \end{bmatrix}. \tag{8}$$

III. Simulations and Discussion

Exponential type of correlation function was known to better characterize rough soil surfaces than Gaussian type [29], [30]. An exponential correlation function contains more high-frequency components than its Gaussian counterpart and, hence, is more suitable for characterizing soil surfaces bearing small-scale details. However, the scale size of surface details much shorter than wavelength can still not be detected. In addition, not all soil surfaces bear small-scale details. For example, it was hypothesized in [29] that the surfaces measured during the first few days after plowing would be more exponential-like, and would become more Gaussian-like after several rain events. In [29], an indicator was defined to determine whether the measured surface topography was more like exponential or Gaussian. In [30], one of the soil samples turned out to fit better with an exponential correlation function while another sample fit better with a Gaussian correlation function. For the convenience of validating our method of computing the brightness temperatures from a layered medium with rough surfaces and spatially varying temperature distribution, two Gaussian type of surfaces from [21], [31] were adopted. It can also be applied to rough surfaces with exponential correlation function.

Both a half-space moistured soil and a two-layered moistured soil are simulated. In the first case, consider a half-space with relative permittivity $\epsilon_r = 17 - j2$. A Gaussian type of rough surface is characterized with correlation length $\ell_c = \lambda$ and rms height $h_{\text{rms}} = 0.1\lambda$. The frequency of the incident field is $f_c = 1.4$ GHz ($\lambda = 21.41$ cm), and the physical temperature of the soil is $T = 300$ K.

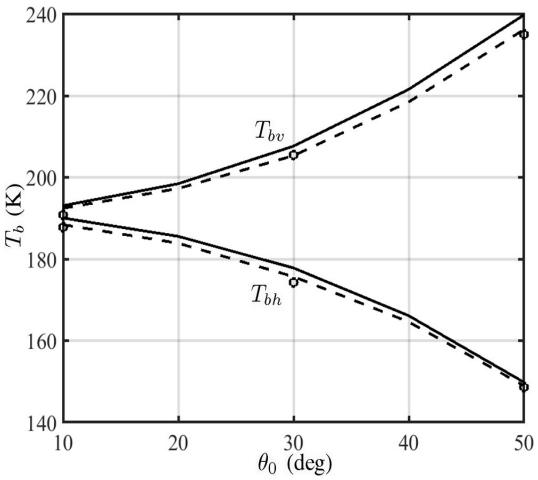

Fig. 2. Brightness temperatures from half-space moistured soil with Gaussian rough surfaces, $f_c = 1.4$ GHz, $\epsilon_r = 17 - j2$, $T = 300$ K, $(h_{\text{rms}}, \ell_c) = (0.1\lambda, \lambda)$. Solid line: proposed method, $L_x = L_y = 8\lambda$, averaged over six realizations; dashed line: near-field BTC [27]; ○: MoM [31].

Fig. 2 shows the brightness temperatures from the half-space moistured soil with rough surface. In the proposed method, T_{bh} and T_{bv} are simulated over six Monte Carlo realizations. The differences of T_{bh} between the proposed method and the MoM [31] at $\theta_0 = 10°, 30°$, and $50°$ are 2.3, 3.5, and 1.2 K, respectively. The differences of T_{bv} between the proposed method and the MoM [31] at $\theta_0 = 10°, 30°$, and $50°$ are 2.2, 2.1, and 4.7 K, respectively. In [31], 1% error (3-K error versus 300 K of physical temperature) was considered acceptable. The errors of T_{bh} at $\theta_0 = 30°$ and T_{bv} at $\theta_0 = 50°$ are 3.5 K (1.2%) and 4.7 K (1.6%), which are slightly above the threshold of 1%.

In this case, the same FDTD scheme is used to compute the fields for the follow-up computation of brightness temperatures with the coherent method and the near-field BTC method, respectively. The major difference between the proposed coherent method and near-field BTC/MoM lies in that the former takes the volume fields in the soil to compute the brightness temperatures, while both the latter takes the surface fields, where the MoM computes the surface fields by using different method than FDTD. The errors in the FDTD scheme may come from the PML reflection, numerical dispersion, incidence tapering, and so on. The integration of volume fields in the FDTD computational domain may accumulate more errors than the near-field BTC method, although the fields used in the two methods come from the same FDTD scheme. Averaging the results over more Monte Carlo realizations of the rough surface does narrow down the difference, but not significant.

In the second case, a two-layered moistured soil with rough interfaces [21] is simulated. The frequency of the incident field is $f = 1.2$ GHz ($\lambda = 0.25$ m). The mean levels of the two rough surfaces are at $z = 0$ and $z = -h_1 = -0.8\lambda$, respectively, where $h_1 = 0.8\lambda$ is considered the thickness of

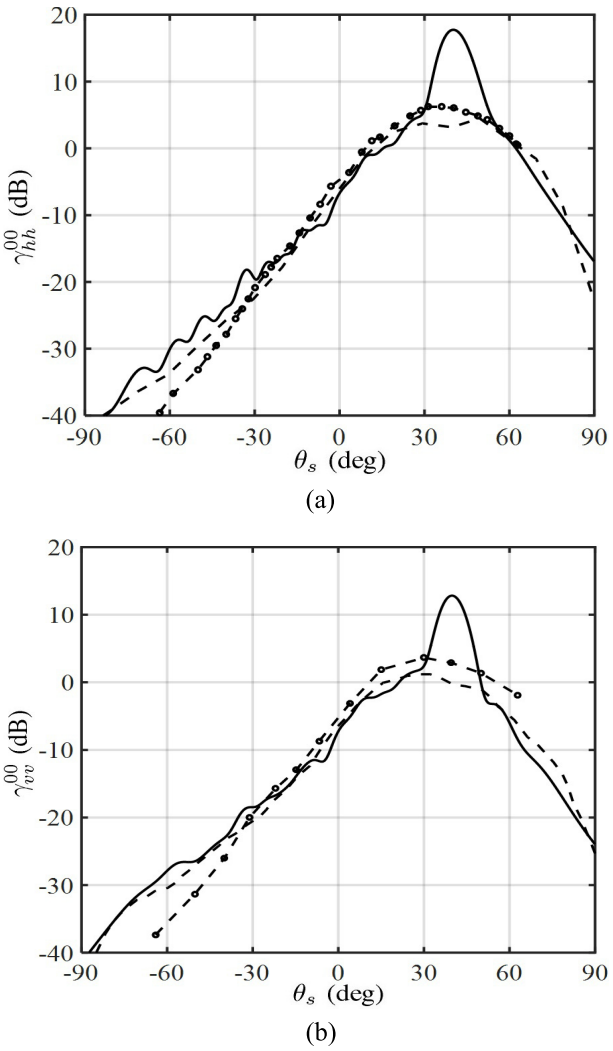

Fig. 3. Copolarized BSCs from two-layered moistured soil with Gaussian rough surfaces. (a) γ_{hh}^{00}. (b) γ_{vv}^{00}. $f_c = 1.2$ GHz, $\theta_i = 40°$, $h_1 = 0.8\lambda$, $\epsilon_{r1} = 5.4 - j0.44$, $\epsilon_{r2} = 11.27 - j$, $(h_{\text{rms1}}, \ell_{c1}) = (0.1\lambda, \lambda)$ and $(h_{\text{rms2}}, \ell_{c2}) = (0.05\lambda, 0.5\lambda)$. Solid line: BSC averaged over 20 realizations with FDTD method, $L_x = L_y = 10\lambda$, $a = 0.1$. Dashed line: incoherent part of BSC averaged over 64 realizations with MoM [21], $L_x = L_y = 16\lambda$. $-\circ-$: incoherent part of BSC with SEBCM [21], $L_x = L_y = 10\lambda$.

the middle layer. The two Gaussian type of rough surfaces are characterized by the rms height and correlation function of $(h_{\text{rms1}}, \ell_{c1}) = (0.1\lambda, \lambda)$ and $(h_{\text{rms2}}, \ell_{c2}) = (0.05\lambda, 0.5\lambda)$, respectively. The relative permittivities in layers (1) and (2) are $\epsilon_{r1} = 5.4 - j0.44$ and $\epsilon_{r2} = 11.27 - j$, respectively, in the L-band, based on the dielectric model in [32] and [33], assuming the volumetric moisture contents of 5% and 14.7%, respectively, with 48% sand and 23% clay. The effective wavelengths are $\lambda_1 = \lambda/\text{Re}\{\sqrt{\epsilon_{r1}}\} = 0.430\lambda = 0.107$ m and $\lambda_2 = \lambda/\text{Re}\{\sqrt{\epsilon_{r2}}\} = 0.298\lambda = 0.074$ m. The equivalent conductivities are $\sigma_1 = \omega\epsilon''_{r1}\epsilon_0 = 0.029$ S/m and $\sigma_2 = \omega\epsilon''_{r2}\epsilon_0 = 0.067$ S/m. The skin depths are $\delta_1 = (2/\omega\mu_0\sigma_1)^{1/2} = 0.085$ m $= 0.34\lambda$ and $\delta_2 = (2/\omega\mu_0\sigma_2)^{1/2} = 0.056$ m $= 0.22\lambda$. The size of Yee cells is chosen to be smaller than 0.1 times the shortest wavelength in the two media. The size of rough surfaces in the computational domain is chosen to be $L_x = L_y = 10\lambda$.

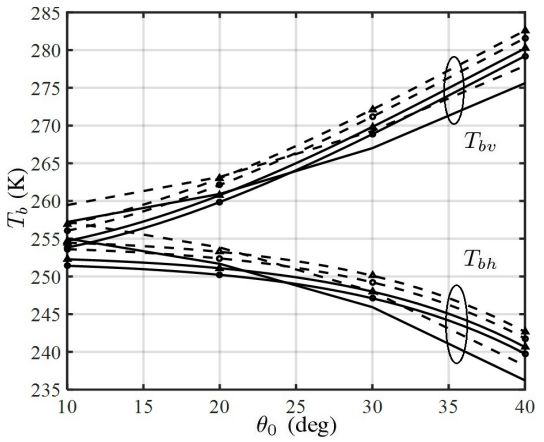

Fig. 4. Brightness temperatures from two-layered moistured soil with rough surfaces, averaged over five realizations with FDTD method. $\epsilon_{r1} = 5.4 - j0.44$, $\epsilon_{r2} = 11.27 - j$, $h_1 = 0.8\lambda$, $(h_{\text{rms1}}, \ell_{c1}) = (0.1\lambda, \lambda)$, $(h_{\text{rms2}}, \ell_{c2}) = (0.05\lambda, 0.5\lambda)$. Dashed line: rough surfaces with FDTD method, $L_x = L_y = 10\lambda$, $T_1 = T_2 = 300$ K. Solid line: rough surfaces with FDTD method, $L_x = L_y = 10\lambda$, $T_1 = 300$ K, $T_2 = 293$ K. $--\circ--$: flat surfaces with analytical coherent method, UPW incidence, $T_1 = T_2 = 300$ K. ——○——: flat surfaces with analytical coherent method, UPW incidence, $T_1 = 300$ K, $T_2 = 293$ K. $--\triangle--$: flat surfaces with analytical coherent method, TPW incidence, $L_x = L_y = 10\lambda$, $T_1 = T_2 = 300$ K. ——△——: flat surfaces with analytical coherent method, TPW incidence, $L_x = L_y = 10\lambda$, $T_1 = 300$ K, $T_2 = 293$ K.

Fig. 3 shows the copolarized BSCs, γ_{hh}^{00} and γ_{vv}^{00}. Each BSC computed with the proposed method is composed of a coherent part and an incoherent part, and those with MoM and SEBCM contain only an incoherent part. It is observed that the coherent part of BSCs appears in an angular range of about 20°, centered at the specular direction of $\theta_s = 40°$. The incoherent part of BSCs with the proposed method agrees well with those by using MoM and SEBCM.

Fig. 4 shows the brightness temperatures from a two-layered moistured soil with rough surfaces, averaged over five realizations with the FDTD method. In most airborne or space-borne measurements, $\bar{r}_0$ in (1) lies in the far-field region, thus the incident field in the computational domain is well approximated as a UPW in theory, which is further approximated as a TPW in the FDTD scheme. The fields computed with the FDTD scheme in the computational domain, which are near fields with respect to the incident plane-wave, are substituted into (1) to compute the brightness temperatures.

For comparison, the brightness temperatures from the same two-layered medium but flat surfaces are also computed by using the analytical coherent method with UPW and TPW, respectively, as the incident wave. The physical temperatures in the two layers are $T_1 = T_2 = 300$ K in case 1 and $T_1 = 300$ K, $T_2 = 293$ K in case 2. It is observed that the brightness temperatures in case 2 are lower than those in case 1 by about 2 K, whether the surfaces are flat or rough. In the case of flat surfaces, the brightness temperatures with TPW are higher than those with UPW by about 1 K. The brightness temperatures with rough surfaces are higher than those with flat surfaces by about 3 K at $\theta_0 = 10°$, and the differences gradually decrease as θ_0 increases. Similar observations appear in [34, Fig. 17], where a half-space medium

below an exponentially correlated surface was simulated with AIEM. Note that layer 2 has a thickness of $h_2 = 4.2\lambda$, which is thick enough for applying the coherent method. By using the proposed method, the difference of brightness temperatures with $h_2 = 4.2\lambda$ and those with $h_2 \to \infty$ is less than 0.5 K.

IV. Conclusion

A coherent method is proposed to compute the brightness temperatures from a half-space moistured soil and a two-layered moistured soil embedding rough surfaces, with the FDTD method to compute the field distribution within the soil. The major contribution of the proposed method lies in its flexibility to compute the brightness temperatures from a layered medium with rough interfaces and spatially varying physical temperature. The brightness temperatures obtained with the proposed method are verified with data in the literature.

References

[1] Y. H. Kerr and E. G. Njoku, "A semiempirical model for interpreting microwave emission from semiarid land surfaces as seen from space," *IEEE Trans. Geosci. Remote Sens.*, vol. 28, no. 3, pp. 384–393, May 1990.

[2] S. Prakash, H. Norouzi, M. Azarderakhsh, R. Blake, and K. Tesfagiorgis, "Global land surface emissivity estimation from AMSR2 observations," *IEEE Geosci. Remote Sens. Lett.*, vol. 13, no. 9, pp. 1270–1274, Sep. 2016.

[3] D. J. Leroux *et al.*, "Active–passive disaggregation of brightness temperatures during the SMAPVEX12 campaign," *IEEE Trans. Geosci. Remote Sens.*, vol. 54, no. 12, pp. 6859–6867, Dec. 2016.

[4] L. Tsang *et al.*, "Active and passive vegetated surface models with rough surface boundary conditions from NMM3D," *IEEE J. Sel. Topics Appl. Earth Obser. Remote Sens.*, vol. 6, no. 3, pp. 1698–1709, Jun. 2013.

[5] F. Jonard, L. Weihermuller, K. Z. Jadoon, M. Schwank, H. Vereecken, and S. Lambot, "Mapping field-scale soil moisture with L-band radiometer and ground-penetrating radar over bare soil," *IEEE Trans. Geosci. Remote Sens.*, vol. 49, no. 8, pp. 2863–2875, Aug. 2011.

[6] Y. H. Kerr *et al.*, "The SMOS mission: New tool for monitoring key elements of the global water cycle," *Proc. IEEE*, vol. 98, no. 5, pp. 666–687, May 2010.

[7] D. Entekhabi *et al.*, "The soil moisture active passive (SMAP) mission," *Proc. IEEE*, vol. 98, no. 5, pp. 704–716, May 2010.

[8] M. C. Dobson, F. T. Ulaby, M. T. Hallikainen, and M. A. El-Rayes, "Microwave dielectric behavior of wet soil—Part II: Dielectric mixing models," *IEEE Trans. Geosci. Remote Sens.*, vol. GE-23, no. 1, pp. 35–46, Jan. 1985.

[9] M. Owe, R. A. M. de Jeu, and T. R. H. Holmes, "Multisensor historical climatology of satellite-derived global land surface moisture," *J. Geophys. Res.*, vol. 113, no. F1, p. F01002, Mar. 2008.

[10] J. Zeng, Z. Li, Q. Chen, and H. Bi, "Method for soil moisture and surface temperature estimation in the Tibetan Plateau using spaceborne radiometer observations," *IEEE Geosci. Remote Sens. Lett.*, vol. 12, no. 1, pp. 97–101, Jan. 2015.

[11] T. Mo, B. J. Choudhury, T. J. Schmugge, J. R. Wang, and T. J. Jackson, "A model for microwave emission from vegetation-covered fields," *J. Geophys. Res.*, vol. 87, no. C13, pp. 11229–11237, Dec. 1982.

[12] J. Y. Zeng, Z. Li, Q. Chen, and H. Y. Bi, "A simplified physically-based algorithm for surface soil moisture retrieval using AMSR-E data," *Frontiers Earth Sci.*, vol. 8, no. 3, pp. 427–438, Sep. 2014.

[13] M. A. Goodberlet and J. B. Mead, "A model of surface roughness for use in passive remote sensing of bare soil moisture," *IEEE Trans. Geosci. Remote Sens.*, vol. 52, no. 9, pp. 5498–5505, Sep. 2014.

[14] R. Panciera, J. P. Walker, and O. Merlin, "Improved understanding of soil surface roughness parameterization for L-band passive microwave soil moisture retrieval," *IEEE Geosci. Remote Sens. Lett.*, vol. 6, no. 4, pp. 625–629, Oct. 2009.

[15] R. D. Lange, R. Beck, N. V. D. Giesen, J. Friesen, A. D. Wit, and W. Wagner, "Scatterometer-derived soil moisture calibrated for soil texture with a one-dimensional water-flow model," *IEEE Trans. Geosci. Remote Sens.*, vol. 46, no. 12, pp. 4041–4049, Dec. 2008.

[16] V. Mironov, Y. Kerr, J.-P. Wigneron, L. Kosolapova, and F. Demontoux, "Temperature- and texture-dependent dielectric model for moist soils at 1.4 GHz," *IEEE Geosci. Remote Sens. Lett.*, vol. 10, no. 3, pp. 419–423, May 2013.

[17] R. T. Shin and J. A. Kong, "Radiative transfer theory for active remote sensing of two-layer random medium," *Prog. Electromag. Res.*, vol. 1, pp. 359–417, 1989. [Online]. Available: http://www.jpier.org/PIER/pier.php?volume=01

[18] S. Mudaliar, "Some issues with using radiative transfer approach to scattering from layered random media with rough interfaces," *IEEE Trans. Antennas Propag.*, vol. 57, no. 11, pp. 3646–3654, Nov. 2009.

[19] A. Tabatabaeenejad and M. Moghaddam, "Study of validity region of small perturbation method for two-layer rough surfaces," *IEEE Geosci. Remote Sens. Lett.*, vol. 7, no. 2, pp. 319–323, Apr. 2010.

[20] J. A. Kong, *Electromagnetic Wave Theory*. Hoboken, NJ, USA: Wiley, 1990.

[21] X. Duan and M. Moghaddam, "Bistatic vector 3-D scattering from layered rough surfaces using stabilized extended boundary condition method," *IEEE Trans. Geosci. Remote Sens.*, vol. 51, no. 5, pp. 2722–2733, May 2013.

[22] X. Duan and M. Moghaddam, "Full-wave electromagnetic scattering from rough surfaces with buried inhomogeneities," *IEEE Trans. Geosci. Remote Sens.*, vol. 55, no. 6, pp. 3338–3353, Jun. 2017.

[23] L. Tsang, *Scattering of Electromagnetic Waves: Numerical Simulations*. Hoboken, NJ, USA: Wiley, 2001, p. 70.

[24] L. Tsang, J. A. Kong, and K.-H. Ding, *Scattering of Electromagnetic Waves: Theory and Applications*, vol. 1. Hoboken, NJ, USA: Wiley, 2001.

[25] K. S. Chen, T.-D. Wu, L. Tsang, Q. Li, J. Shi, and A. K. Fung, "Emission of rough surfaces calculated by the integral equation method with comparison to three-dimensional moment method simulations," *IEEE Trans. Geosci. Remote Sens.*, vol. 41, no. 1, pp. 90–101, Jan. 2003.

[26] L. He, L. Lang, Q. Li, and W. Zheng, "Effect of surface roughness on microwave brightness temperature from lunar surface: Numerical analysis with a hybrid method," *Adv. Space Res.*, vol. 51, pp. 179–187, Jan. 2013.

[27] Z.-H. Lai and J.-F. Kiang, "Brightness temperatures from very lossy medium with near-field bistatic transmission coefficients," *IEEE Trans. Geosci. Remote Sens.*, vol. 57, 2019.

[28] Z.-H. Lai, J.-F. Kiang, and R. Mittra, "A domain decomposition finite difference time domain (FDTD) method for scattering problem from very large rough surfaces," *IEEE Trans. Antennas Propag.*, vol. 63, no. 10, pp. 4468–4476, Oct. 2015.

[29] M. Schwank *et al.*, "Comparison of two bare-soil reflectivity models and validation with L-band radiometer measurements," *IEEE Trans. Geosci. Remote Sens.*, vol. 48, no. 1, pp. 325–337, Jan. 2010.

[30] Y. Oh, K. Sarabandi, and F. T. Ulaby, "An empirical model and an inversion technique for radar scattering from bare soil surfaces," *IEEE Trans. Geosci. Remote Sens.*, vol. 30, no. 2, pp. 370–381, Mar. 1992.

[31] Q. Li, L. Tsang, K. S. Pak, and C. H. Chan, "Bistatic scattering and emissivities of random rough dielectric lossy surfaces with the physics-based two-grid method in conjunction with the sparse-matrix canonical grid method," *IEEE Trans. Antennas Propag.*, vol. 48, no. 1, pp. 1–11, Jan. 2000.

[32] N. R. Peplinski, F. T. Ulaby, and M. C. Dobson, "Dielectric properties of soils in the 0.3–1.3-GHz range," *IEEE Trans. Geosci. Remote Sens.*, vol. 33, no. 3, pp. 803–807, May 1995.

[33] P. C. Dubois, J. vanZyl, and T. Engman, "Corrections to 'Measuring soil moisture with imaging radars,'" *IEEE Trans. Geosci. Remote Sens.*, vol. 33, no. 6, p. 1340, Nov. 1995.

[34] J. Zeng, K.-S. Chen, H. Bi, T. Zhao, and X. Yang, "A comprehensive analysis of rough soil surface scattering and emission predicted by AIEM with comparison to numerical simulations and experimental measurements," *IEEE Trans. Geosci. Remote Sens.*, vol. 55, no. 3, pp. 1696–1708, Mar. 2017.